Journal of Advanced Ceramics
2017, **6**(2): 81–89
DOI: 10.1007/s40145-017-0220-x

ISSN 2226-4108
CN 10-1154/TQ

Research Article

Color tunable $Ba_{0.79}Al_{10.9}O_{17.14}$:*x*Eu phosphor prepared in air via valence state control

Ziyao WANG, Yangai LIU*, Jian CHEN, Minghao FANG, Zhaohui HUANG, Lefu MEI

Beijing Key Laboratory of Materials Utilization of Nonmetallic Minerals and Solid Wastes, *National Laboratory of Mineral Materials*, *School of Materials Science and Technology*, *China University of Geosciences*, *Beijing 100083*, *China*

Received: December 24, 2016; Revised: February 26, 2017; Accepted: February 27, 2017

Abstract: A series of luminescent $Ba_{0.79}Al_{10.9}O_{17.14}$:*x*Eu ($x = 0.005$–$0.12$) phosphors were prepared by high-temperature solid-state reaction in air atmosphere. The coexistence of Eu^{2+} and Eu^{3+} was observed and verified by photoluminescence (PL) and photoluminescence excitation (PLE) spectra, X-ray photoelectron spectra (XPS), and diffuse reflection spectra. The band emission peaking at 430 nm was assigned to $4F^6 5D–4F^7$ transition of Eu^{2+}, and another four emissions peaking at 589, 619, 655, and 704 nm were attributed to 4F–4F transitions of $^5D_0$–^7F_J ($J = 1, 2, 3, 4$) of Eu^{3+}. The related mechanism of self-reduction was discussed in detail. The color of the $Ba_{0.79}Al_{10.9}O_{17.14}$:*x*Eu phosphors could be shifted from blue (0.23, 0.10) to red (0.42, 0.27) by doping Li^+ ions, and the temperature dependence properties were investigated.

Keywords: tunable; phosphor; $Ba_{0.79}Al_{10.9}O_{17.14}$; luminescence; self-reduction

1 Introduction

White light emitting diode (WLED) is considered as a new generation of solid-state lighting source due to the characteristics of high energy efficiency, long lifetime, low energy consumption, etc. There are three traditional approaches to generate WLED: (1) YAG phosphor excited by blue LED, (2) direct white phosphor excited by ultraviolet (UV) LED, and (3) tricolor phosphor excited by near ultraviolet (NUV) LED. The third approach pumping blue, green, and red emitting phosphors with NUV LED deserves more attention because it displays extensive spectral distribution over the whole visible range to obtain high quality white light [1–5]. Hexagonal aluminates have good thermal and chemical stabilities, which are widely used as tricolor phosphor host materials [6,7]. The luminescence property of Eu^{2+} and Ce^{3+} doped $BaAl_{12}O_{19}$ was firstly studied by Verstegen and Stevels [8] in 1974. Xiao *et al*. [9] reported the effects of crystallization temperature, Eu^{2+} concentration, and Al^{3+} content on the occupation of Eu^{2+} in $BaAl_{12}O_{19}$:Eu^{2+} phosphor. The energy transfer mechanisms in $BaAl_{12}O_{19}$:Ce^{3+},Eu^{2+} phosphor were investigated in detail by Jeon *et al*. [10]. Deshmukh *et al*. [11] reported the effect of Ca^{2+} and Sr^{2+} ions on luminescence properties of $BaAl_{12}O_{19}$:Eu^{2+} phosphor. $BaAl_{12}O_{19}$ also can be used as long afterglow phosphor with co-doped Eu and Dy and shows high brightness, long afterglow time, and stable performance [12].

Generally, Eu^{2+} ions are usually used as an activator

* Corresponding author.
E-mail: liuyang@cugb.edu.cn

of the blue luminescent materials because of the predominant $4F^6 5D–4F^7$ transition peaking from 400 to 550 nm [13,14]. With the wide use of Eu_2O_3 as raw material in the synthesis of Eu-doped phosphors, the most common method to obtain Eu^{2+} is preparing under reducing atmosphere, such as H_2, H_2/N_2, or C. Since the reduction process from Eu^{3+} to Eu^{2+} in air was first found by non-equivalent substitution method in the 1990s [15], many reports pointed out that the reduction of Eu^{3+} to Eu^{2+} happens in some particular hosts in air atmosphere. In 1998, Zeng *et al*. [16] reported the reduction of Eu^{3+} in SrB_6O_{10} prepared in air and the luminescence of SrB_6O_{10}:Eu^{3+}. Next year, Pei *et al*. [17] discussed the mechanism of the abnormal reduction of Eu^{3+} to Eu^{2+} in $Sr_2B_5O_9Cl$. Subsequently, Peng *et al*. [18,19] observed the emission of Eu^{3+} and Eu^{2+} in $BaMgSiO_4$ and $Sr_4Al_{14}O_{25}$ prepared in air in 2003. Compared with traditional reactions, the novel way for the preparation of Eu^{2+} is of great importance for safe production, process simplifying, and cost reducing. As reported by Chen *et al*. [20] and Lian *et al*. [21], there are four conditions are essential for the self-reduction of Eu^{3+} to Eu^{2+}: (1) no oxidizing ions in the hosts; (2) bivalent cations in the hosts substituted by Eu^{3+} ions; (3) similar radius between substituted cation and Eu^{2+} ion; and (4) appropriate tetrahedron anion structures in the hosts.

Up to now, there are not any related reports about $Ba_{0.79}Al_{10.9}O_{17.14}$:Eu prepared in air. In this study, a series of tunable $Ba_{0.79}Al_{10.9}O_{17.14}$:Eu phosphors were prepared in air by high-temperature solid-state reaction. The coexistence of Eu^{2+} and Eu^{3+} was proved by photoluminescence spectra, diffuse reflection spectra, and X-ray photoelectron spectra. The self-reduction mechanism was discussed in detail based on the charge compensation model, and the reduction process could be controlled by tuning synthesis temperature and doping concentration of Eu^{3+} and Li^+ ions to obtain the colorful tunable phosphor.

2 Experimental

$Ba_{0.79}Al_{10.9}O_{17.14}$ host, Eu^{3+} ion single-doped samples $Ba_{0.79}Al_{10.9}O_{17.14}$:$x$Eu ($x$ = 0.005, 0.01, 0.02, 0.04, 0.06, 0.08, 0.10, 0.12), and co-doped samples $Ba_{0.79}Al_{10.9}O_{17.14}$:0.04Eu,$y$$Li^+$ (y = 0.04, 0.06, 0.08, 0.10, 0.12, 0.14) were synthesized by conventional solid-state reaction in air with $BaCO_3$ (analytical reagent), Al_2O_3 (analytical reagent), Li_2CO_3 (analytical reagent), and Eu_2O_3 (4N). The stoichiometric amounts of raw materials were well homogenized in an agate mortar. All samples were pre-sintered in air at 900 ℃ for 3 h, and further heat treated at 1300 ℃ for 3 h. Finally, three samples of $Ba_{0.79}Al_{10.9}O_{17.14}$:0.04Eu were calcined at 1500 ℃, 1550 ℃, 1600 ℃ for 3 h respectively, and the other samples were calcined at 1550 ℃ for 5 h to complete reaction with several intermediate grindings in the processes.

The phase composition of synthesized samples was analyzed by X-ray diffraction (XRD) on a D8 Advance diffractometer with Cu Kα1 radiation (λ = 1.5406 Å) by the step of 4 (°)/min at room temperature. The emission and excitation spectra, and the temperature dependant luminescence properties were detected with a Hitachi F-4600 fluorescence spectrophotometer. The diffuse reflection spectra were measured via a Shimadzu UV-3600 UV–Vis–NIR spectrophotometer attached with an integral sphere. The photoluminescence decay curves were determined by a Horiba JOBIN YVON FL3-21 spectrofluorometer.

3 Results and discussion

3.1 Crystal structures

Figure 1 shows the XRD patterns of $Ba_{0.79}Al_{10.9}O_{17.14}$ synthesized at 1450 ℃, $Ba_{0.79}Al_{10.9}O_{17.14}$:0.04Eu synthesized at 1450 ℃, 1500 ℃, 1550 ℃, and $Ba_{0.79}Al_{10.9}O_{17.14}$:0.04Eu,0.04$Li^+$ synthesized at 1550 ℃ for 4 h in air. The reference pattern of the standard JCPDS Card No. 77-1522 for $Ba_{0.79}Al_{10.9}O_{17.14}$ was also listed in Fig. 1 in the bottom. It is indicated that the samples prepared in different conditions are all in pure $Ba_{0.79}Al_{10.9}O_{17.14}$ phase, and the changes of synthesis temperature and doping of Eu^{3+} ions would not impact the host structure. When Li^+ ions were doped into the $Ba_{0.79}Al_{10.9}O_{17.14}$ host, the main diffraction peaks shifted slightly to higher angles. The change indicates that the Li^+ ions replace the ions with comparatively small radii in the $Ba_{0.79}Al_{10.9}O_{17.14}$ host lattice.

The fragments of $Ba_{0.79}Al_{10.9}O_{17.14}$ unit cell are exhibited in Fig. 2. $Ba_{0.79}Al_{10.9}O_{17.14}$ is hexagonal structure with space group $P6_3/mmc$, in which the Ba^{2+} ions occupy nine-coordinated sites, and the Al^{3+} ions form tetrahedrons and octahedrons with different

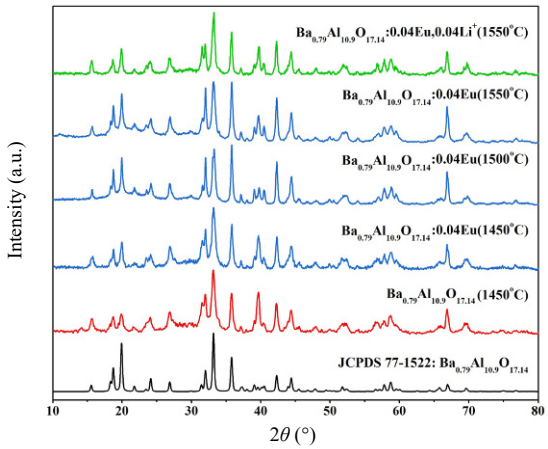

Fig. 1 XRD patterns of $Ba_{0.79}Al_{10.9}O_{17.14}$, $Ba_{0.79}Al_{10.9}O_{17.14}$:0.04Eu, and $Ba_{0.79}Al_{10.9}O_{17.14}$:0.04Eu,0.04$Li^+$ synthesized at different temperatures.

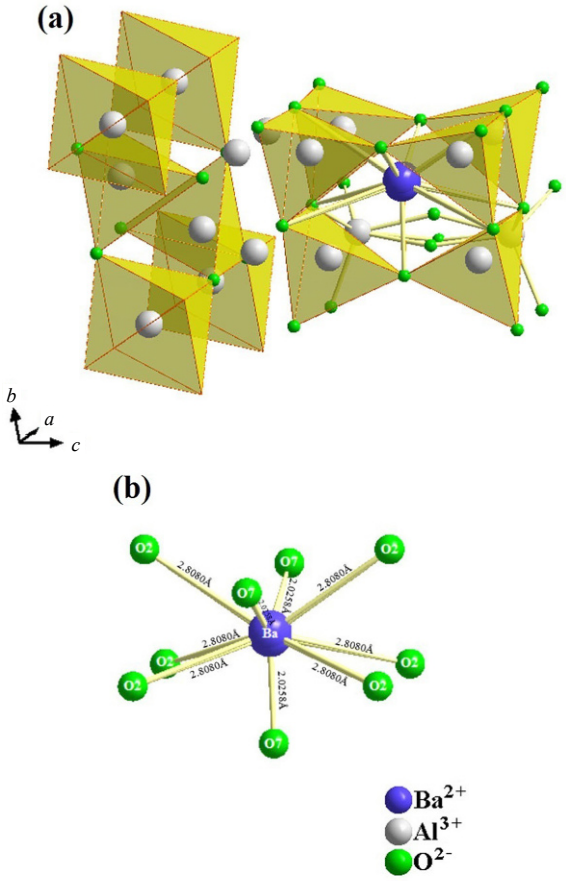

Fig. 2 Crystal structures of $Ba_{0.79}Al_{10.9}O_{17.14}$.

coordinations [22]. The radius difference between Ba^{2+} and Eu^{2+} is much smaller than that of Ba^{2+} and Eu^{3+} as well as Ba^{2+} and Al^{3+} [23,24]. Thus, it is reasonable to consider the Eu ions are substituted in the Ba^{2+} ion sites. Considering the charge mismatching between Ba^{2+} and Eu^{3+}, the Eu^{3+} ions are introduced into the Ba^{2+} sites in a non-equivalent compensation way.

3. 2 Self-reduction of Eu^{3+} to Eu^{2+} in $Ba_{0.79}Al_{10.9}O_{17.14}$:*x*Eu

The photoluminescence excitation (PLE) and photoluminescence (PL) spectra of $Ba_{0.79}Al_{10.9}O_{17.14}$: 0.04Eu are shown in Fig. 3. It is found that there is a coexistence of Eu^{2+} and Eu^{3+} in the host after sintering at 1550 ℃ for 4 h, though the source of Eu ions is Eu_2O_3. Monitoring the characteristic excitation of two ions, as shown in Fig. 3(a), the broad absorption bands monitored at 431 nm peaking at 259 and 314 nm originate from $4F^7$–$4F^65D$ transitions of Eu^{2+}, while the other absorption band monitored at 619 nm peaking at 254 nm is attributed to the ^7F_J (J=1, 2, 3, 4)–$^5D_0$ transitions of Eu^{3+} [25]. The PL spectra under varying excitation factors are shown in Fig. 3(b). The luminescence characteristics of Eu^{2+} and Eu^{3+} are both observed in emission spectra under different excitations. The band emission peaking at 431 nm is assigned to $4F^65D$–$4F^7$ transition of Eu^{2+}, and the other six typical line emissions peaking at 578, 589, 600, 619, 655, and

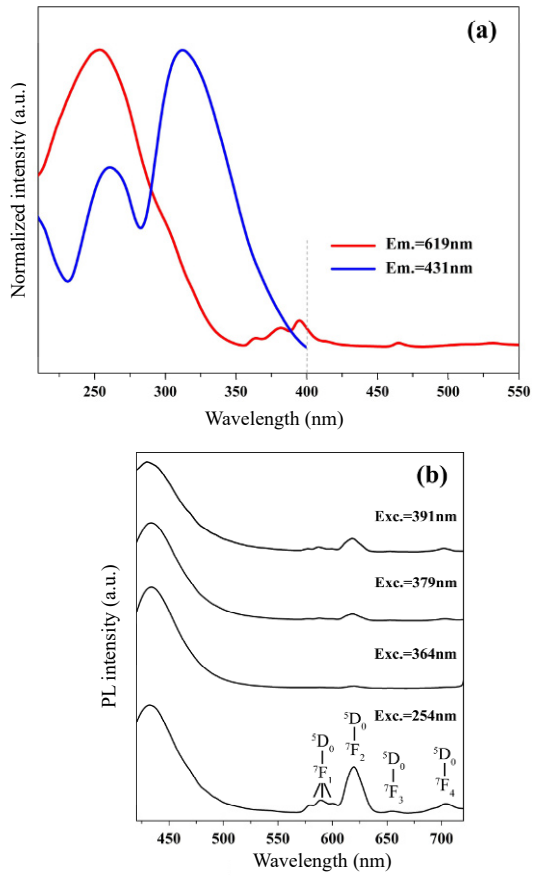

Fig. 3 (a) PLE spectra of Eu^{3+} (619 nm) and Eu^{2+} (431 nm) emissions of $Ba_{0.79}Al_{10.9}O_{17.14}$:0.04Eu and (b) PL spectra with different excitation factors.

706 nm are attributed to 4F–4F transitions of $^5D_0$–^7F_J (J = 1, 2, 3, 4) of Eu^{3+}.

As we know, $^5D_0$–$^7F_{1,3}$ of Eu^{3+} belong to the magnetic dipole transitions, whereas $^5D_0$–$^7F_{2,4}$ are electric dipole transitions [26]. The strongest emission peaking at 619 nm from $^5D_0$–$^7F_2$ transition of Eu^{3+} reflects that the electric dipole transition is the dominant factor, which is greatly influenced by the lattice symmetry [27].

Figure 4 presents the diffuse reflection spectra of $Ba_{0.79}Al_{10.9}O_{17.14}$:$x$Eu ($x$ = 0–0.10). It is observed that the energy absorption of $Ba_{0.79}Al_{10.9}O_{17.14}$ host appears in UV range, and the band gap is about 3.37 eV, which is estimated by the fitting line of the absorption edge. With Eu^{3+} ions doping into the host, a broad absorption band occurs around 200–300 nm in the near-UV region because of the $4F^7$–$4F^65D$ transition from Eu^{2+}, and another one weak absorption peaking at 391 nm originates from the transition $^7F_3$–$^5D_0$ from Eu^{3+}, which is in accordance with the excitation spectra of Eu^{2+} and Eu^{3+}, indicating that Eu^{2+} and Eu^{3+} can be singly or both excited with the various excitation wavelengths.

The coexistence of Eu^{2+} and Eu^{3+} ions is also pointed out by X-ray photoelectron spectra (XPS), as shown in Fig. 5. Only one broad band peaking at 1136.5 eV is observed when the preparation temperatures are 1450 ℃ and 1500 ℃, which is ascribed to Eu^{3+} $3d_{5/2}$, because the self-reaction is incomplete and the amount of Eu^{2+} is limited at this point. And another one peak at 1127.5 eV consistent with Eu^{2+} $3d_{5/2}$ is observed as the preparation temperature rises to 1550 ℃ [28].

The charge compensation model is an important theory for explaining the reduction of Eu^{3+} to Eu^{2+} in $Ba_{0.79}Al_{10.9}O_{17.14}$:$x$Eu in air [29–31]. It is known that the Eu^{3+} ions occupy the Ba^{2+} sites in a non-equivalent compensation way, and every three Ba^{2+} ions are substituted by two Eu^{3+} ions for balancing the charge

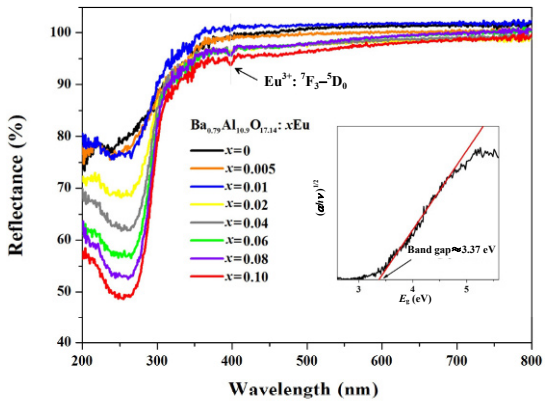

Fig. 4 Diffuse reflection spectra of $Ba_{0.79}Al_{10.9}O_{17.14}$:$x$Eu ($x$ = 0–0.10).

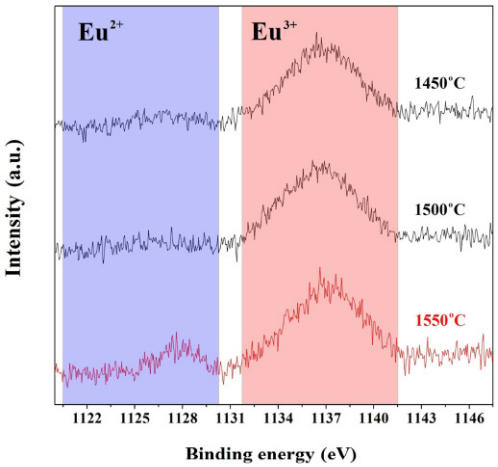

Fig. 5 High-resolution XPS spectra of the Eu 3d peaks of $Ba_{0.79}Al_{10.9}O_{17.14}$:0.04Eu.

neutrality. Thus one vacancy defect of V''_{Ba} with two negative charges and two positively charged defects of Eu_{Ba} are created. The vacancy works as the donor of electrons, while the defect works as the acceptor of electrons in the host. Thermal effect promotes the transition of negative charges from vacancy of V''_{Ba} to Eu^{3+} sites. When the negative charges get to the Eu^{3+} sites, they will fill into the 4F orbit of Eu ions. As a consequence, the Eu^{3+} ions are reduced to Eu^{2+} ions in air. According to the electroneutrality principle [32,33], the doped Li^+ ions, working as the charge compensators, neutralize the negative charges and occupy the Ba vacancies. They prevent the formation of new vacancies, and promote the reaction going towards the reactants. The reaction process is conducted as follows:

$$3Ba^{2+} + 2Eu^{3+} \rightarrow V''_{Ba} + 2Eu_{Ba} \quad (1)$$

$$V''_{Ba} \rightarrow V^{x}_{Ba} + 2e \quad (2)$$

$$2Eu_{Ba} + 2e \rightarrow 2Eu^{x}_{Ba} \quad (3)$$

When Eu^{3+} ions are doped into the host and reduced to Eu^{2+} ions, they will be surrounded by the framework structure of AlO_4 tetrahedron, which has considerable inhibitory effects on oxidation of Eu^{2+} [34,35]. The framework consists of six-membered network structures formed by corner-shared AlO_4 tetrahedrons, whose centers are occupied by Eu^{2+} ions working as the charge compensation cations. The Eu^{2+} ions in the hollow structures of AlO_4 tetrahedrons are protected from oxidation, so that they can exist stably in the host.

3.3 Luminescence of $Ba_{0.79}Al_{10.9}O_{17.14}$:$x$Eu

The amount ratio of Eu^{2+} and Eu^{3+} ions in the host is defined as η, which can approximately be equal to the

proportion of emission intensity at 431 and 619 nm. Figure 6 presents the PL spectra ($\lambda_{ex}=254$ nm) of $Ba_{0.79}Al_{10.9}O_{17.14}$:$x$Eu ($x=0.005$–$0.12$) prepared at 1550 ℃ for 4 h and the variation of η with the variety of the Eu^{3+} ion concentration. The emissions of Eu^{2+} and Eu^{3+} enhance with the increase of Eu^{3+} ion concentration and reach the maximum at 2 mol% due to the concentration quenching [36,37]. The value of η has a similar tendency with emission intensity which indicates that the Eu^{2+} emission of blue light plays a leading role when the concentration of Eu^{3+} ions is changed from 0.5 to 12 mol%, and the small amount doping of Eu^{3+} ions can promote the self-reduction to some extent.

The decay curves of the Eu^{2+} and Eu^{3+} luminescence in $Ba_{0.79}Al_{10.9}O_{17.14}$:$x$Eu ($x=0.04$–$0.12$) prepared at 1550 ℃ upon excitation at 359 and 375 nm are measured and depicted in Fig. 7. The corresponding lifetime can be well fitted to a first-order exponential equation [20]:

$$I(t)=A\exp(-t/\tau) \tag{4}$$

where I is the luminescence intensity, A is a constant, t is the time, and τ is the lifetime for the exponential component. As shown in Fig. 7(a), the lifetime excited at 359 nm and monitored at 431 nm is determined to be 1599.20, 1554.25, 1543.08, 1509.84, and 1444.31 ns with the Eu concentrations $x=0.04$, 0.06, 0.08, 0.10, 0.12, respectively. The obtained result demonstrates the measured lifetime τ of Eu^{2+} 5D–4F emission decreases with the increasing concentration of Eu^{2+}, and the concentration quenching effect occurs. It is found from Fig. 7(b) that the lifetime monitored at 619 nm with different Eu^{3+} concentrations is 1.08, 1.06, 1.01, 0.98, 0.96 ms, respectively. The lifetime τ of Eu^{3+} 4F–4F

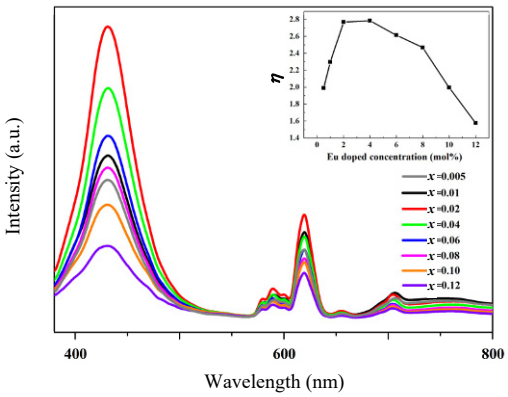

Fig. 6 PL spectra and dependence of η on the amount of Eu in $Ba_{0.79}Al_{10.9}O_{17.14}$:$x$Eu ($x=0.005$–$0.12$) prepared at 1550 ℃ for 4 h.

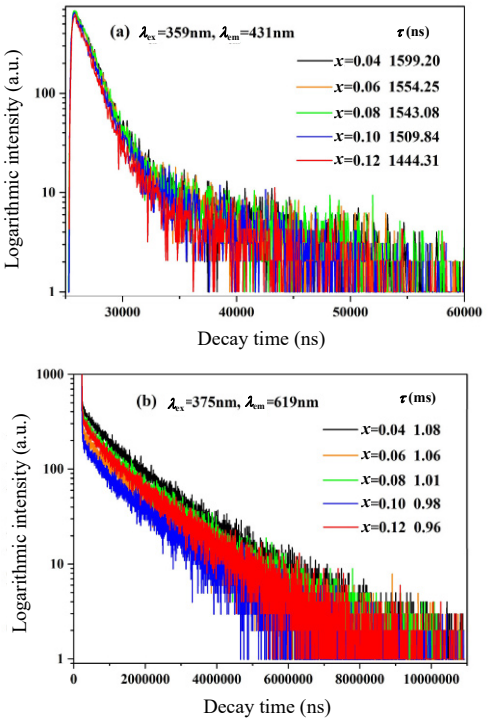

Fig. 7 Decay curves of $Ba_{0.79}Al_{10.9}O_{17.14}$:$x$Eu ($x=0.04$–$0.12$) monitored at (a) 431 and (b) 619 nm.

emission decreases with the increase in Eu^{3+} concentration. The calculated lifetime is also fitted to the equation of the total relaxation rate [38,39]:

$$\frac{1}{\tau}=\frac{1}{\tau_0}+A_{nr}+P_t \tag{5}$$

where τ_0 is the relative lifetime, A_{nr} is the non-radiative rate due to multiphonon relaxation, and P_t is the energy transfer rate between Eu^{3+} ions. With increasing of Eu^{3+} ions, the distance between Eu^{3+} ions decreases, and the energy transfer rate among Eu^{3+} and the probability of energy transfer to luminescent killer sites increase. Therefore, the lifetime is shorten with increasing Eu^{3+} concentration [40].

With the increasing doping of Li^{+} ions, as shown in Fig. 8, the calculated lifetime of Eu^{2+} decreases and the reaction goes towards the reactants. It can be indicated that the content of Eu^{3+} increases, and the energy transfer process between Eu^{2+} and Eu^{3+} is enhanced.

Figure 9 displays the PL spectra of $Ba_{0.79}Al_{10.9}O_{17.14}$: 0.04Eu prepared at 1450 ℃, 1500 ℃, and 1550 ℃ for 4 h, and the variation of η with different preparation temperatures is shown in the inset. It is found that η is increased with the rise of synthesis temperature, and the emission intensity of Eu^{2+} increases while the emission intensity of Eu^{3+} decreases obviously. When the

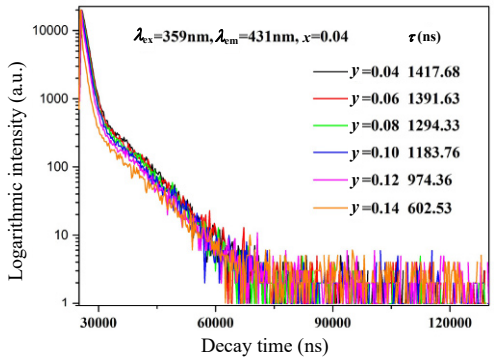

Fig. 8 Decay curves of $Ba_{0.79}Al_{10.9}O_{17.14}$:0.04Eu,$yLi^+$ (y = 0.04–0.14) monitored at 431 nm.

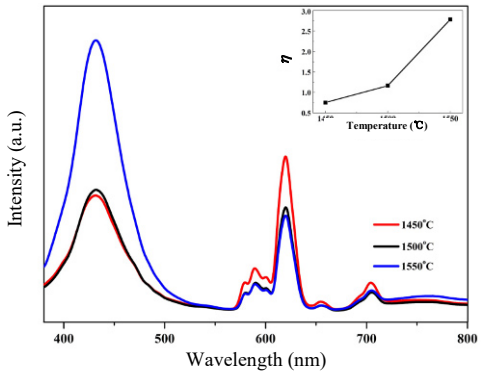

Fig. 9 PL spectra and dependence of η on the synthesis temperature (1450 ℃, 1500 ℃, 1550 ℃) of $Ba_{0.79}Al_{10.9}O_{17.14}$: 0.04Eu for 4 h.

synthesis temperature is less than 1500 ℃, Eu^{3+} emission of red light is the dominant effect. Eu^{2+} emission becomes dominant when the synthesis temperature increases above 1500 ℃. The result indicates that the preparation temperature rise can be an advantage for self-reduction of Eu^{3+}.

The PL spectra of $Ba_{0.79}Al_{10.9}O_{17.14}$:0.04Eu,$yLi^+$ (y = 0.04–0.14) prepared at 1550 ℃ for 4 h and the variation of η are illustrated in Fig. 10. It is found the blue emissions of Eu^{2+} are very sensitive with the doping of Li^+ ions which play a role of charge compensation. Both the emission intensity of Eu^{2+} and the value of η decrease with the increase of Li^+ ion doping concentration, because self-reduction of Eu^{3+} goes towards the reactants. Figure 11 shows the CIE chromaticity diagram of $Ba_{0.79}Al_{10.9}O_{17.14}$:0.04Eu,$yLi^+$ (y = 0.04–0.14) and the relative digital images upon excitation of 254 nm. It can be concluded that the doping of Li^+ ions promotes the self-reduction of Eu^{3+} ions, and the color of phosphors can be shifted from blue (0.23, 0.10) to red (0.42, 0.27).

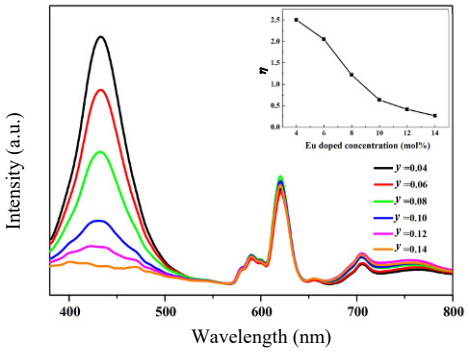

Fig. 10 PL spectra and dependence of η on the amount of Li^+ in $Ba_{0.79}Al_{10.9}O_{17.14}$:0.04Eu,$yLi^+$ (y = 0.04–0.14) prepared at 1550 ℃ for 4 h.

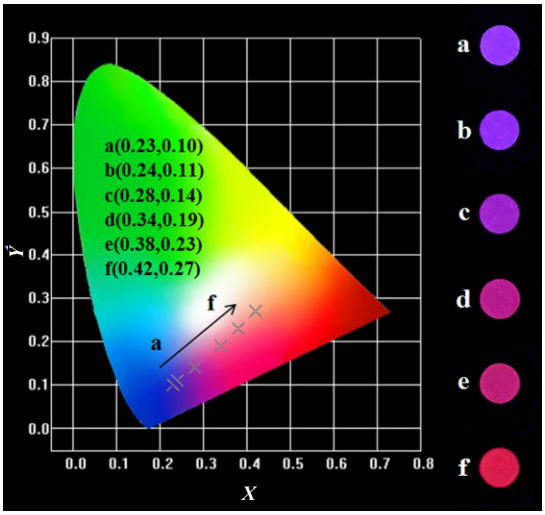

Fig. 11 CIE chromaticity diagram of $Ba_{0.79}Al_{10.9}O_{17.14}$: 0.04Eu,$yLi^+$ (y = 0.04–0.14) and digital images in UV box.

3. 4 Temperature dependence properties

It is known that the thermal quenching property is an important factor for white light output in white LED application [41,42]. The temperature-dependent emission spectra (λ_{ex} = 254 nm) of $Ba_{0.79}Al_{10.9}O_{17.14}$: 0.04Eu,0.04Li$^+$ prepared in air are shown in Figs. 12(a) and 12(b). The emission intensity decreases to 83.84% at 100 ℃ and 70.73% at 150 ℃ compared with the intensity at room temperature, which indicates that the $Ba_{0.79}Al_{10.9}O_{17.14}$:0.04Eu,0.04Li$^+$ phosphor shows good thermal stability. The decrease of emission intensity is due to the probability of molecule collision and nonradiative transition is enhanced with the temperature rise [43].

The activation energy from the temperature quenching can be calculated with the Arrhenius equation [44,45]:

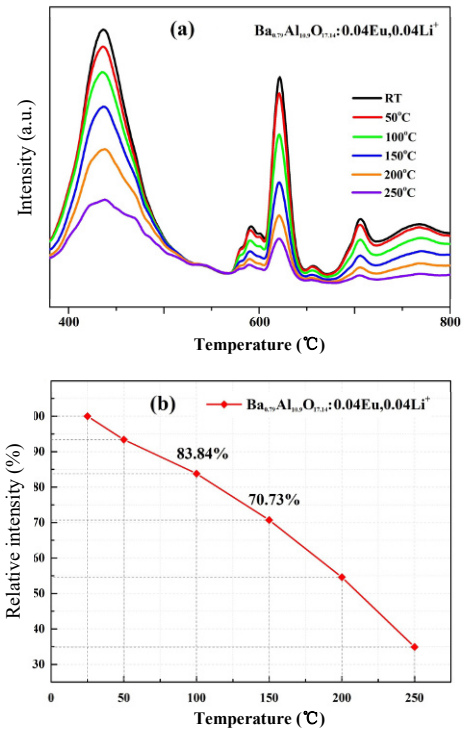

Fig. 12 (a) Temperature-dependent emission spectra of $Ba_{0.79}Al_{10.9}O_{17.14}$:0.04Eu,0.04Li$^+$ and (b) emission intensity function relative to the temperature.

$$I_T = \frac{I_0}{1 + c\exp\left(-\frac{\Delta E}{kT}\right)} \tag{6}$$

where I_0 is the emission intensity of $Ba_{0.79}Al_{10.9}O_{17.14}$:0.04Eu,0.04Li$^+$ phosphor at room temperature, I_T is the emission intensity at different temperature, c is a constant, ΔE is the activation energy for temperature quenching, k is the Boltzman's constant (8.62×10^{-5} eV), and T is the temperature. As Fig. 13 shows, the relationship between $1/(kT)$ and $\ln(I_0/I-1)$ presents a relative linearity, and the activation energy for thermal quenching of $Ba_{0.79}Al_{10.9}O_{17.14}$:0.04Eu,0.04Li$^+$ is calculated as 0.232 eV. The slope of the straight line is –0.232 which equals to $-\Delta E$.

4 Conclusions

Tunable luminescent $Ba_{0.79}Al_{10.9}O_{17.14}$:$x$Eu ($x$ = 0.005–0.12) phosphors have been prepared successfully in air by high-temperature solid-state reaction. The coexistance of Eu^{2+} and Eu^{3+} in the host has been observed, and the mechanism of self-reduction has been discussed in detail based on the charge compensation

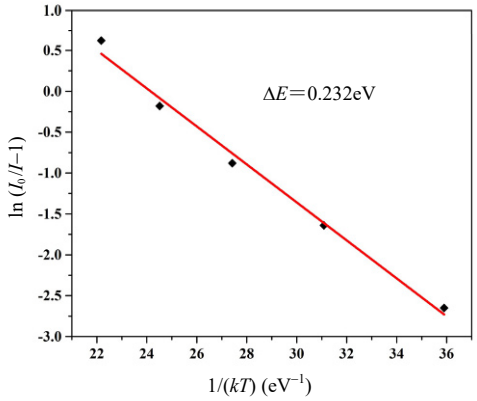

Fig. 13 Arrhenius fitting of the emission intensity of $Ba_{0.79}Al_{10.9}O_{17.14}$:0.04Eu,0.04Li$^+$ and the calculated activation energy (ΔE) for thermal quenching.

model. The critical quenching concentration of Eu^{2+} in $Ba_{0.79}Al_{10.9}O_{17.14}$:$x$Eu ($x$ = 0.005–0.12) is about 2 mol%, which is verified to be the dipole–dipole interaction. The colors of phosphors can be easily tuned from blue (0.23, 0.10) to red (0.42, 0.27) by adjusting the valance state through controlling the concentration of Li^+, and the emission intensity maintains at a high level with 70.73% at 150 ℃ compared with the intensity at room temperature. The prepared $Ba_{0.79}Al_{10.9}O_{17.14}$:$x$Eu ($x$ = 0.005–0.12) phosphors can be regarded as an alternative to obtain color tunable emission for white LED.

Acknowledgements

We thank the National Natural Science Foundation of China (Grant No. 51472223), the Program for New Century Excellent Talents in University of Ministry of Education of China (Grant No. CET-12-0951), and the Fundamental Research Funds for Central Universities (Grant No. 2652015090).

References

[1] Wang M-S, Guo S-P, Li Y, *et al*. A direct white-light-emitting metal–organic framework with tunable yellow-to-white photoluminescence by variation of excitation light. *J Am Chem Soc* 2009, **131**: 13572–13573.

[2] Cao R, Xiong Q, Luo W, *et al*. Synthesis and luminescence properties of efficient red phosphors $SrAl_4O_7$:Mn^{4+},R^+ (R^+ = Li^+, Na^+, and K^+) for white LEDs. *Ceram Int* 2015, **41**: 7191–7196.

[3] Chen J, Liu Y-G, Mei L, *et al*. Emission red shift and energy transfer behavior of color-tunable $KMg_4(PO_4)_3$: Eu^{2+},Mn^{2+} phosphors. *J Mater Chem C* 2015, **3**: 5516–5523.

[4] Zhao X, Ding Y, Li Z, *et al*. An efficient charge compensated red phosphor Sr_3WO_6:K^+,Eu^{3+}—For white LEDs. *J Alloys Compd* 2013, **553**: 221–224.

[5] Xia Z, Zhou J, Mao Z. Near UV-pumped green-emitting $Na_3(Y,Sc)Si_3O_9$:Eu^{2+} phosphor for white-emitting diodes. *J Mater Chem C* 2013, **1**: 5917–5924.

[6] Singh V, Sivaramaiah G, Rao JL, *et al*. Optical and EPR properties of $BaAl_{12}O_{19}$:Eu^{2+},Mn^{2+} phosphor prepared by facile solution combustion approach. *J Lumin* 2015, **157**: 74–81.

[7] Ravichandran D, Johnson ST, Erdei S, *et al*. Crystal chemistry and luminescence of the Eu^{2+}-activated alkaline earth aluminate phosphors. *Displays* 1999, **19**: 197–203.

[8] Verstegen JMPJ, Stevels ALN. The relation between crystal structure and luminescence in β-alumina and magnetoplumbite phases. *J Lumin* 1974, **9**: 406–414.

[9] Xiao L, He M, Tian Y, *et al*. Study on luminescence properties of Eu^{2+} in $BaAl_{12}O_{19}$ matrix. *J Nanosci Nanotechno* 2010, **10**: 2131–2134.

[10] Jeon HS, Kim SK, Park HL, *et al*. Observation of two independent energy transfer mechanisms in $BaAl_{12}O_{19}$: $Ce^{3+}_{0.06} + Eu^{2+}_{x}$ phosphor. *Solid State Commun* 2001, **120**: 221–225.

[11] Deshmukh AD, Dhoble SJ, Dhoble NS. Optical properties of $MAl_{12}O_{19}$:Eu (M = Ca, Ba, Sr) nanophosphors. *Adv Mat Lett* 2011, **2**: 38–42.

[12] Xiong Y, Wang Y-H, Hu Z-F, *et al*. Luminescence properties of Eu,Dy doped $BaAl_{12}O_{19}$ long afterglow phosphors. *Spectrosc Spect Anal* 2012, **32**: 614–618.

[13] Mi R, Zhao C, Xia Z. Synthesis, structure, and tunable luminescence properties of novel $Ba_3NaLa(PO_4)_3F$: Eu^{2+},Mn^{2+} phosphors. *J Am Ceram Soc* 2014, **97**: 1802–1808.

[14] Kim JS, Jeon PE, Choi JC, *et al*. Warm-white-light emitting diode utilizing a single-phase full-color $Ba_3MgSi_2O_8$:Eu^{2+},Mn^{2+} phosphor. *Appl Phys Lett* 2004, **84**: 2931–2933.

[15] Pei Z, Su Q. The valence change from RE^{3+} to RE^{2+} (RE = Eu, Sm, Yb) in SrB_4O_7:RE prepared in air and the spectral properties of RE^{2+}. *J Alloys Compd* 1993, **198**: 51–53.

[16] Zeng Q, Pei Z, Wang S, *et al*. The reduction of Eu^{3+} in SrB_6O_{10} prepared in air and the luminescence of SrB_6O_{10}:Eu. *J Alloys Compd* 1998, **275–277**: 238–241.

[17] Pei Z, Zeng Q, Su Q. A study on the mechanism of the abnormal reduction of Eu^{3+}→Eu^{2+} in $Sr_2B_5O_9Cl$ prepared in air at high temperature. *J Solid State Chem* 1999, **145**: 212–215.

[18] Peng M, Pei Z, Hong G, *et al*. The reduction of Eu^{3+} to Eu^{2+} in $BaMgSiO_4$:Eu prepared in air and the luminescence of $BaMgSiO_4$:Eu^{2+} phosphor. *J Mater Chem* 2003, **13**: 1202–1205.

[19] Peng M, Pei Z, Hong G, *et al*. Study on the reduction of Eu^{3+}→Eu^{2+}, in $Sr_4Al_{14}O_{25}$:Eu prepared in air atmosphere. *Chem Phys Lett* 2003, **371**: 1–6.

[20] Chen J, Liu Y, Liu H, *et al*. Tunable $SrAl_2Si_2O_8$:Eu phosphor prepared in air via valence state-controlled means. *Opt Mater* 2015, **42**: 80–86.

[21] Lian Z, Wang J, Lv Y, *et al*. The reduction of Eu^{3+} to Eu^{2+} in air and luminescence properties of Eu^{2+} activated $ZnO–B_2O_3–P_2O_5$ glasses. *J Alloys Compd* 2007, **430**: 257–261.

[22] Singh V, Chakradhar RPS, Rao JL, *et al*. Luminescence and EPR studies of Eu^{2+} doped $BaAl_{12}O_{19}$ blue light emitting phosphors. *J Lumin* 2010, **130**: 703–708.

[23] Peng M, Qiu J, Yang I, *et al*. Observation of Eu^{3+}→Eu^{2+} in barium hexa-aluminates with β' or β-alumina structures prepared in air. *Opt Mater* 2004, **27**: 591–595.

[24] Chen J, Liu Y, Liu H, *et al*. The luminescence properties of novel α-$Mg_2Al_4Si_5O_{18}$:Eu^{2+} phosphor prepared in air. *RSC Adv* 2014, **4**: 18234–18239.

[25] Peng M, Hong G. Reduction from Eu^{3+} to Eu^{2+} in $BaAl_2O_4$:Eu phosphor prepared in an oxidizing atmosphere and luminescent properties of $BaAl_2O_4$:Eu. *J Lumin* 2007, **127**: 735–740.

[26] Dhoble SJ, Raut SK, Dhoble NS. Synthesis and photoluminescence characteristics of rare earth activated some silicate phosphors for LED and display devices. *International Journal of Luminescence and Applications* 2015, **5**: 178–182.

[27] Parchur AK, Ningthoujam RS. Behaviour of electric and magnetic dipole transitions of Eu^{3+}, $^5D_0$→$^7F_0$ and Eu–O charge transfer band in Li^+ co-doped YPO_4: Eu^{3+}. *RSC Adv* 2012, **2**: 10859–10868.

[28] Swart HC, Terblans JJ, Ntwaeaborwa OM, *et al*. Applications of AES, XPS and TOF SIMS to phosphor materials. *Surf Interface Anal* 2014, **46**: 1105–1109.

[29] Liu S, Zhao G, Ruan W, *et al*. Reduction of Eu^{3+} to Eu^{2+} in aluminoborosilicate glasses prepared in air. *J Am Ceram Soc* 2008, **91**: 2740–2742.

[30] Shi S, Gao J, Zhou J. Effects of charge compensation on the luminescence behavior of Eu^{3+} activated $CaWO_4$ phosphor. *Opt Mater* 2008, **30**: 1616–1620.

[31] Li YQ, de With G, Hintzen H. Luminescence properties of Ce^{3+}-activated alkaline earth silicon nitride $M_2Si_5N_8$ (M = Ca, Sr, Ba) materials. *J Lumin* 2006, **116**: 107–116.

[32] Gruber B. *Theory of Crystal Defects*. New York: Academia Press, 1966.

[33] Zhang ZW, Wang XJ, Ren YJ. Enhanced red emission in $Ca_{2.96}Eu_{0.04}(PO_4)_2$ phosphor by charge compensation. *Chinese Journal of Luminescence* 2014, **35**: 1071–1075. (in Chinese)

[34] Su Q, Zeng QH, Pei ZW. Preparation of borates doped with divalent rare earth ions (RE^{2+}) in air and spectroscopy of divalent rare earth ions (RE^{2+} = Sm, Eu, Tm, Yb). *Chinese Journal of Inorganic Chemistry* 2000, **16**: 293–298. (in Chinese)

[35] Rezende MVS, Valerio MEG, Jackson RA. Study of Eu^{3+}→Eu^{2+} reduction in $BaAl_2O_4$:Eu prepared in different gas atmospheres. *Mater Res Bull* 2014, **61**: 348–351.

[36] Wang D, Yin Q, Li Y, *et al*. Concentration quenching of Eu^{2+} in $SrO·6Al_2O_3$:Eu^{2+} phosphor. *J Mater Sci* 2002, **37**: 381–383.

[37] Zhou Z, Yu Y, Liu X, *et al*. Luminescence enhancement of $CaMoO_4$:Eu^{3+} phosphor by charge compensation using

microwave sintering method. *J Adv Ceram* 2015, **4**: 318–325.
[38] Blasse G, Wanmaker WL, ter Vrugt JW, *et al*. Fluorescence of Eu^{2+} activated silicates. *Philips Res Rep* 1968, **23**: 189–200.
[39] Henderson B, Imbusch GF. *Optical Spectroscopy of Inorganic Solids*. Clarendon: Clarendon Press, 1989.
[40] Wang D-Y, Huang C-H, Wu Y-C, *et al*. $BaZrSi_3O_9:Eu^{2+}$: A cyan-emitting phosphor with high quantum efficiency for white light-emitting diodes. *J Mater Chem* 2011, **21**: 10818–10822.
[41] Geng D, Li G, Shang M, *et al*. Color tuning via energy transfer in $Sr_3In(PO_4)_3:Ce^{3+}/Tb^{3+}/Mn^{2+}$ phosphors. *J Mater Chem* 2012, **22**: 14262–14271.
[42] Xia Y, Chen J, Liu Y-G, *et al*. Luminescence properties and energy transfer in $K_2MgSiO_4:Ce^{3+},Tb^{3+}$ as a green phosphor. *Mater Express* 2016, **6**: 37–44.
[43] Mi R, Chen J, Liu Y, *et al*. Luminescence and energy transfer of a color tunable phosphor: Tb^{3+} and Eu^{3+} co-doped $ScPO_4$. *RSC Adv* 2016, **6**: 28887–28894.
[44] Xia Z, Liu R-S, Huang K-W, *et al*. $Ca_2Al_3O_6F:Eu^{2+}$: A green-emitting oxyfluoride phosphor for white light-emitting diodes. *J Mater Chem* 2012, **22**: 15183–15189.
[45] Xie R-J, Hirosaki N, Kimura N, *et al*. 2-phosphor-converted white light-emitting diodes using oxynitride/nitride phosphors. *Appl Phys Lett* 2007, **90**: 191101.